Tetherless mobile micrograsping using a magnetic elastic composite material

2016 Smart Mater. Struct. 25 11LT03

(http://iopscience.iop.org/0964-1726/25/11/11LT03)

Letters

IOP Publishing Smart Materials and Structures

Smart Mater. Struct. **25** (2016) 11LT03 (7pp) doi:10.1088/0964-1726/25/11/11LT03

Letter

Tetherless mobile micrograsping using a magnetic elastic composite material

Jiachen Zhang and Eric Diller

Microrobotics Laboratory, Department of Mechanical and Industrial Engineering, Univeristy of Toronto, Toronto, Ontario M5S 3G8, Canada

E-mail: ediller@mie.utoronto.ca

Received 13 April 2016, revised 1 September 2016
Accepted for publication 5 October 2016
Published 24 October 2016

Abstract

In this letter, we propose and characterize a new type of tetherless mobile microgripper for micrograsping that is made of a magnetic elastic composite material. Its magnetically-programmable material and structures make it the first three-dimensional (3D) mobile microgripper that is directly actuated and controlled by magnetic forces and torques. With a symmetric four-limb structure, the microgripper is 3.5 mm long from tip to tip when it is open and 30 μm thick. It forms an approximate 700 μm cube when it is closed. The orientation and 3D shape of the microgripper are determined by the direction and strength of the applied magnetic field, respectively. As a mobile device, the microgripper can be moved through aqueous environments for precise grasping and transportation of micro-objects, pulled by magnetic gradients directly or rolled in rotating magnetic fields. The deformation of the microgripper under magnetic actuation is characterized by modeling and confirmed experimentally. Being directly controlled by magnetic forces and torques, the microgripper is easier and more intuitive to control than other magnetic microgrippers that require other inputs such as thermal and chemical responses. In addition, the microgripper is capable of performing fast repeatable grasping motions, requiring no more than 25 ms to change from fully open to fully closed in water at room temperature. As a result of its large-amplitude 3D deformation, the microgripper can accommodate cargoes with a wide range of geometries and dimensions. A pick-and-place experiment demonstrates the efficacy of the microgripper and its potentials in biomedical, microfluidic, and microrobotic applications.

S Online supplementary data available from stacks.iop.org/sms/25/11LT03/mmedia

Keywords: smart magnetic materials, micro-manipulation, micro-robotics

(Some figures may appear in colour only in the online journal)

1. Introduction

Recent advancement of mobile microrobotics suggests new solutions for tasks in healthcare [1–5] and micro-factory [6–10]. One major challenge in microrobotics is the control and actuation of microrobots, which is not trivial considering that most microrobots do not have space for onboard power or electronic systems. Magnetic field is utilized to provide energy and controlling signals to microrobots, with its distinct advantages of being able to penetrate most materials, especially biological substances, and generate forces and torques on magnetic materials remotely and simultaneously. One disadvantage of magnetic field is that it cannot generate torques around the magnetic moment direction of the microrobot, limiting the maximum number of degree-of-freedom (DOF) of microrobot in three-dimensional (3D) space to be five. Nevertheless, this limitation has been partly solved by Diller *et al* when a non-uniform

magnetization profile is achievable within the microrobot body, enabling full six-DOF actuation [11]. Additionally, the topic of powering and controlling multiple microrobots using a single magnetic field has been widely discussed and many mechanisms have been proposed [12–14]. These merits make magnetic field a popular choice in microrobotic tasks, including swimming [15, 16], microfluidic regulation [10, 17], and microobject manipulation [18–20]. The emerged magnetic microrobots have diverse forms and functionalities, among which the magnetic microgrippers attract much attention as a result of their promising applications in intravascular surgery [21] and micro-object manipulation and/or transportation [7–9]. Many of these magnetic microgrippers are made of soft elastic materials. These soft microgrippers are easy to fabricate, immune to damage, safe in biomedical applications, and capable of performing tasks using their deformable bodies. Although magnetic field can provide energy, other inputs such as thermal [22] and chemical responses [23] are often required to fully control a microgripper: exerting authorities over its orientation, shape, and position. For example, Breger *et al* proposed a soft-bodied microgripper with a tip-to-tip length of ~7 mm that is opened and closed by the environmental temperature change [22]. Involving other responses makes magnetic microgrippers more complex and less efficient. And some of these other responses are harmful to cells and tissues, compromising the bio-compatibility of these microgrippers. Efforts have been made to fully control microgrippers using only magnetic fields. Kuo *et al* designed a two-dimensional (2D) intravascular microgripper that uses magnetic field as its driving source and control signal [21]. Although this microgripper does not require any temperature change of its environment to work, its deformation still relies on a thermal response induced by the applied alternating magnetic field through the Nel and Brownian relaxation process. And it takes the microgripper ten or more seconds to close its grasping tips. Diller and Sitti presented two kinds of 2D tetherless soft-bodied microgrippers actuated by magnetic forces and magnetic torques, respectively [6]. Both kinds of microgrippers are made of soft elastomer with embedded magnetic particles, and fully controlled by magnetic effects without involving any other responses such as thermal or chemical actuation. The torque-based microgripper is successfully demonstrated to perform 3D microassembly. Further study shows this microgripper can pick-and-place microgels into a 3D heterogeneous assembly with up to ten layers [7]. Nevertheless, these microgrippers are 2D and their deformation ranges are relatively small, limiting the geometry and dimension of the cargo they can securely grasp.

Here we present for the first time a 3D tetherless mobile microgripper that is fully controlled by magnetic forces and torques. The microgripper is made of a magnetic elastic composite material, which contains permanent magnetic micro-scale particles in its polymeric matrix. The orientation and shape of the microgripper are determined by the direction and strength of the applied magnetic field, respectively. And the microgripper can be pulled by magnetic forces generated by magnetic field gradient or rolled by magnetic torques in rotating magnetic fields. Thus, the microgripper's grasp-and-release action and translation/rolling motion are uncoupled and can be controlled independently and simultaneously, which is one of its advantages. The microgripper prototype has a tip-to-tip length of 3.5 mm and a thickness of 30 μm. When it is closed, it forms an approximate 700 μm cube. The structure of the microgripper comprises nine magnetic blocks and one nonmagnetic frame. The microgripper closes in strong magnetic fields and opens in weak ones. A model based on the Euler–Bernoullic beam theory is proposed to characterize the relationship between the 3D shape of the microgripper and the strength of the applied magnetic field. The proposed microgripper has the following attractive features besides the common benefits of soft-bodied microrobots. First, it is controlled by a simple setup, i.e., a 3D electromagnetic coil system, and the control principles using magnetic forces and torques are straightforward, simplifying the required control algorithms. Second, its 3D shape can be accurately and quickly changed by varying the strength of the applied magnetic field. Due to its direct magnetic actuation, it is able to perform close-and-open motions up to a speed of 20 Hz. Thus, when the microgripper fails in grasping its cargo or loses it during transportation, more attempts can be made immediately to restore it. Third, the microgripper can be pulled using magnetic field gradients and also rolled in rotating magnetic fields. Pulling is more intuitive to control, while rolling can help the microgripper overcome the friction when it moves on surfaces.

2. Materials and structures

The microgripper is made of a magnetic elastic composite material and has a symmetric 3D structure. The nine magnetic blocks of the microgripper consist of one base, four arms, and four fingers. The arms and the fingers are allocated evenly to four identical and orthogonal limbs around the base that is at the geometric center of the microgripper. Figure 1 shows the structure of the microgripper and its fabrication process.The fabrication has three steps. First, negative molds are made for the blocks and the frame using photolithography (SU-8 2025, MicroChem Corp.) on silicon wafers [7]. Second, a relatively stiff silicone elastomer material (Sylgard 184, Dow Corning) is mixed homogeneously with permanent magnetic particles (MQFP-15-7, NdPrFeB, Magnequench) at a mass ratio of 1:1, after which this mixture is poured into the molds for blocks (figure 1(c)). After this mixture has cured, the blocks are taken out from their molds and magnetized differently based on their positions in the microgripper. Two permanent magnets (N40, Magnet4US) creates a strong uniform magnetic field of 1.1 T in the 3 mm gap between them (figure 1(g)). For magnetization, a block is mounted on an acrylic stage at a predefined tilting angle β, and then inserted into the strong magnetic field. The magnetic particles in the block are magnetized, resulting in constant magnetization across the block's body. The tilting angle β equals to the angle from a block's surface to its magnetization and is therefore referred to as the

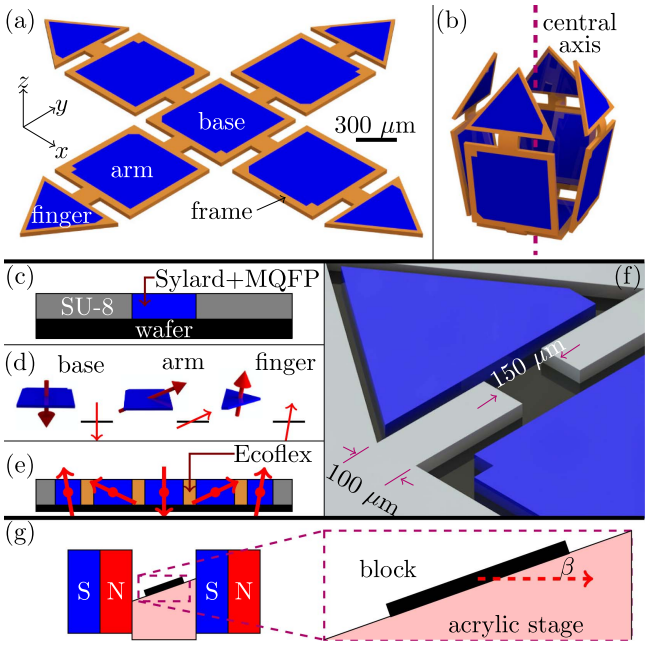

Figure 1. Schematics of the microgripper and its fabrication process. Different parts of the microgripper are labeled in (a) and its shape in an applied magnetic field is shown in (b) The magnetic blocks are fabricated from their corresponding negative molds (c) and magnetized differently by a strong magnetic field created by two permanent magnets (g). The magnetization profiles of blocks are different based on their positions in the microgripper (d). These magnetized blocks are placed in the frame mold ((e) and (f)), from which the nonmagnetic frame is fabricated. The red arrows in (d) and (e) stand for the magnetization direction.

magnetization angle β: $\beta_{\text{base}} = -90°$, $\beta_{\text{arm}} = 25°$, and $\beta_{\text{finger}} = 80°$ (figure 1(d)). These β angles are chosen to close the microgripper in an applied magnetic field along the central axis. Third, the magnetized blocks are placed in the mold for the frame (figures 1(e) and (f)), and one type of highly flexible elastomer (Ecoflex 00-50, Smooth-On) fills this mold to connect neighboring blocks. After the frame has cured, the microgripper is taken out from the mold manually using tweezers. In an applied magnetic field, the relatively stiff blocks experience magnetic forces and torques and work as the 'bones' of the microgripper, while the flexibility of the frame makes it easy to bend and suitable for the functionality of 'soft joints'. Consequently, the microgripper possesses the necessary stiffness to securely grasp its cargo and the required flexibility to deform easily in magnetic field.

3. Characterization

The behavior of the microgripper is determined by its material properties (stiffness and magnetization), its structural geometry, and the applied magnetic field. Magnetic particles in the elastic composite experience forces $\mathbf{F}$ and torques $\boldsymbol{\tau}$ in the applied magnetic field $\mathbf{B}$ as

$$\mathbf{F} = (\mathbf{m} \cdot \nabla)\mathbf{B} \tag{1}$$

and

$$\boldsymbol{\tau} = \mathbf{m} \times \mathbf{B}, \tag{2}$$

where $\mathbf{m}$ and $\mathbf{B}$ are the magnetic moment and the magnetic flux density, respectively. The force is nonzero when the field is not uniform, and the torque exists until the particle's magnetic moment is aligned with the field direction. In this work, magnetic force is used to move the microgripper by pulling, while magnetic torque makes the microgripper grasp. For convenience, the magnetization direction of the base block is defined as the microgripper's positive direction. When magnetic field is absent, the microgripper remains stationary and fully open, exhibiting a close-to-zero net magnetic moment. From this state, if a magnetic field is applied along the microgripper's positive direction, the microgripper's limbs will bend in the positive direction and the microgripper will close. On the contrary, if the applied field is along the negative direction, the microgripper's limbs will deform towards its negative direction and make itself a 'bowl' shape. After the microgripper closes or forms a 'bowl', its net magnetic moment increases along its central axis, and magnetic torque will always align the microgripper with the magnetic field. This alignment enables a different locomotion style, i.e., the microgripper rolls on a surface when the magnetic field rotates.

To characterize the shape of the microgripper, the actuating magnetic torques need to be calculated first. Since the magnetization within a block is equal everywhere, the magnetic torque $\boldsymbol{\tau}$ on one block is

$$\boldsymbol{\tau} = (\mathbf{M} \times \mathbf{B})V, \tag{3}$$

where $\mathbf{M}$ and V are the magnetization and the volume of this block, respectively. When the central axis of the microgripper is aligned with the applied magnetic field, the four limbs of the microgripper will be curled up by the magnetic torques and the microgripper closes. Thus, the deformation level of the microgripper is controlled by the magnitude of the applied magnetic torque. With the symmetric geometry and magnetization, the four limbs of the microgripper behave identically in theory and similarly in practice. Therefore, the deformation level of the microgripper can be represented by two bending angles α_1 and α_2 in radians defined in figure 2(a). A succinct model based on the Euler–Bernoulli beam theory is proposed to relate the two bending angles to the strength of the applied magnetic field. It is assumed that the deformation only happens at the frame joints, whereas the blocks and the other part of the frame remain undeformed. The joint curvature κ in figure 2(a) is seen as

$$\kappa_i = \frac{\alpha_i}{L_i}, \tag{4}$$

where $i = \{1, 2\}$, and L is the joint's length. The curvature can also be calculated as

$$\kappa_i = \frac{Q_i}{E_i I_i}, \tag{5}$$

where Q, E, and I are the bending moment, the Young's modulus, and the second moment of area, respectively.

Knowing that $E_1 = E_2$ and $I_1 = I_2$, we can combine the two joint curvatures into one equation as

$$\begin{bmatrix}\kappa_1\\ \kappa_2\end{bmatrix} = \frac{1}{EI}\begin{bmatrix}1 & 1\\ 0 & 1\end{bmatrix}\begin{bmatrix}Q_1\\ Q_2\end{bmatrix} \tag{6}$$

and

$$Q_i = |\mathbf{M}||\mathbf{B}|V_i \sin\gamma_i, \tag{7}$$

where $i = \{1,\ 2\}$, and γ is the angle between the magnetization of the corresponding block and the applied magnetic field.

Because the magnetic field is always aligned with the central axis of the microgripper, the angle γ can be calculated geometrically as

$$\begin{bmatrix}\gamma_1\\ \gamma_2\end{bmatrix} = \begin{bmatrix}-1 & 0\\ -1 & -1\end{bmatrix}\begin{bmatrix}\alpha_1\\ \alpha_2\end{bmatrix} + \begin{bmatrix}\beta_{\text{arm}}\\ \beta_{\text{finger}}\end{bmatrix} + \frac{\pi}{2}. \tag{8}$$

Combining (2)–(6), we can merge the variables representing the physical properties of the microgripper into one magneto-flexural rigidity $\eta = |\mathbf{M}|/(EI)$. Assuming η is known and the initial values of α_1 and α_2 are zero, the shape of the microgripper given by κ can be calculated iteratively until a converging value is reached.

Fitting the simulated results to the measurements in a characterization experiment, we estimate the unknown coefficient to be $\eta \approx 6.69 \times 10^{17}\ \text{A}\,\text{N}^{-1}\,\text{m}^{-3}$. In addition, the magnetization value is independently measured to be $|\mathbf{M}| = 47\ \text{kA}\,\text{m}^{-1}$, which is obtained by fitting the magnetic field generated by a polymer block that has the same magnetization amplitude with the microgripper to a magnetic dipole model. With this value of η, the simulated and experimental bending angles are plotted together in figure 2(b). And figure 3 shows a sequence of frames of the microgripper in the characterization experiment, clearly showing that the microgripper closes in strong magnetic fields and opens in weak ones. The agreement between the two data sets suggests that, although the Euler–Bernoullic beam theory does not contain a large-deflection model, it still gives a meaningful approximation of the deformation in our case. In nonuniform magnetic fields, the microgripper experiences magnetic torques and forces simultaneously. But it is observed that the magnetic torque effect dominates over any internal deformation due to magnetic forces. As a result, the 3D shape of the microgripper in nonuniform magnetic fields exhibits a pattern similar with the one in uniform magnetic fields: the microgripper closes in strong magnetic fields and opens in weak ones. Thus, magnetic forces are ignored in the preceding analysis.

Different with many other microgrippers in the literature, the proposed microgripper 'hugs' its cargo, instead of 'pinching' it at a point. This feature enables the microgripper to pick up cargoes with a wide variety of dimensions and geometries. But at the same time, it obscures the analysis of gripping force. A rough estimation shows that each arm and finger can apply forces up to 16 μN and 6 μN on the cargo in a magnetic field of 15 mT, respectively. This estimation is obtained from simulation results and is only expected to give an idea of the magnitude of the gripping force, as the actual force depends on the exact contact conditions. It assumes that the cargo is rigid and fully fills the internal space formed by the microgripper when it closes, forming surface contact with the microgripper's body.

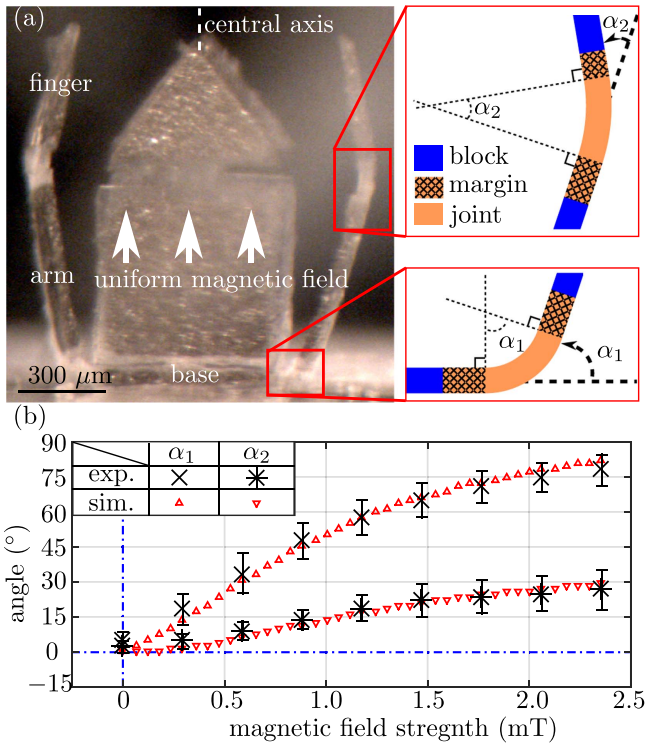

Figure 2. Illustrations and results of the characterization experiment performed in water. A photograph of the microgripper is shown in (a), with schematics of the bending angles α_1 and α_2. Experimental results are compared with the predictions from the model in (b). Each experimental data point is the mean value of 24 measurements (6 times for each limb). The error bar of a data point corresponds to its standard deviation.

4. Experiments and demonstrations

A pick-and-place experiment, in which the microgripper is immersed in water, is presented here to demonstrate the controllability of the microgripper and its potentials in microrobotic applications. The microgripper is actuated and controlled by a magnetic field with controllable magnitude and direction, generated by a 3D electromagnetic coil system (figures 4(a) and (b)) [15]. This system has six coils in three pairs arranged along three orthogonal axes, i.e., x, y and z-axes. Only powering current to one coil of a pair generates field gradient in the workspace along the central axis of this coil pair (figure 4(c)). A uniform magnetic field is achieved if both coils in a pair are powered with currents with the same direction and amplitude, as shown in figure 4(d). The strength of the resultant magnetic field is proportional to the current amplitude. As a result, this system can generate uniform field and also field gradient along an arbitrary 3D direction in its

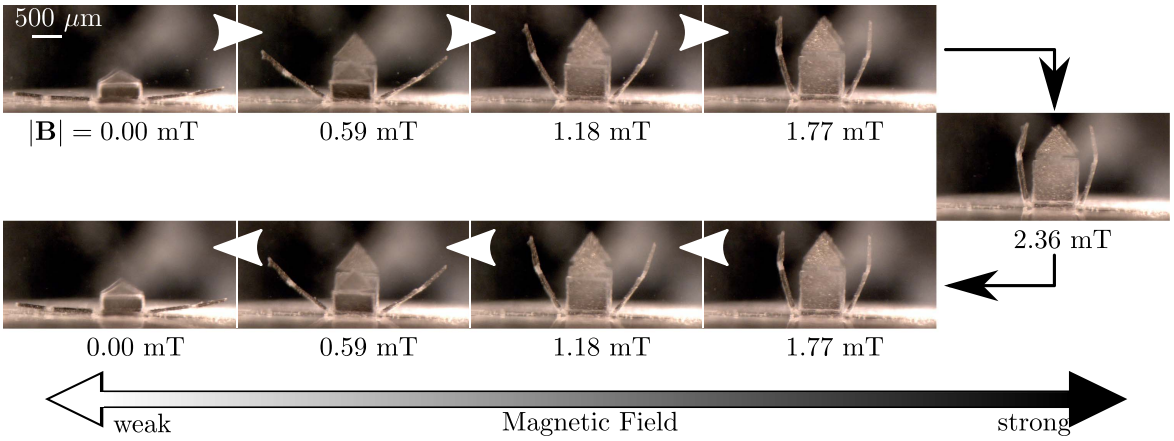

Figure 3. A sequence of frames of the microgripper in the characterization experiment. The arrows between frames indicate the chronological order of the frames.The double arrow at the bottom shows the strength of the applied uniform magnetic field.

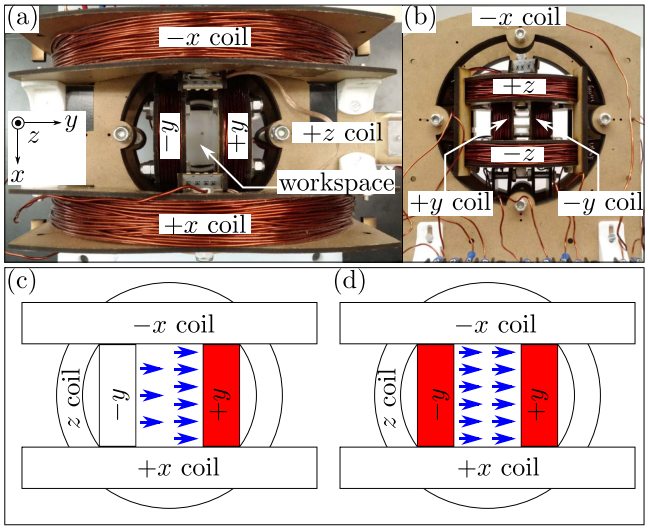

Figure 4. The coil system and schematics showing its working principles. The top view and the side view of the system are shown in (a) and (b), respectively. Magnetic gradient is generated in the workspace when only one coil in a pair is powered, as shown in (c) with red marks the coil with current in it and the density of blue arrows denotes the field strength. Alternatively, powering both coils in a pair with current with the same amplitude in the same direction results in a uniform field in the workspace, as shown in (d).

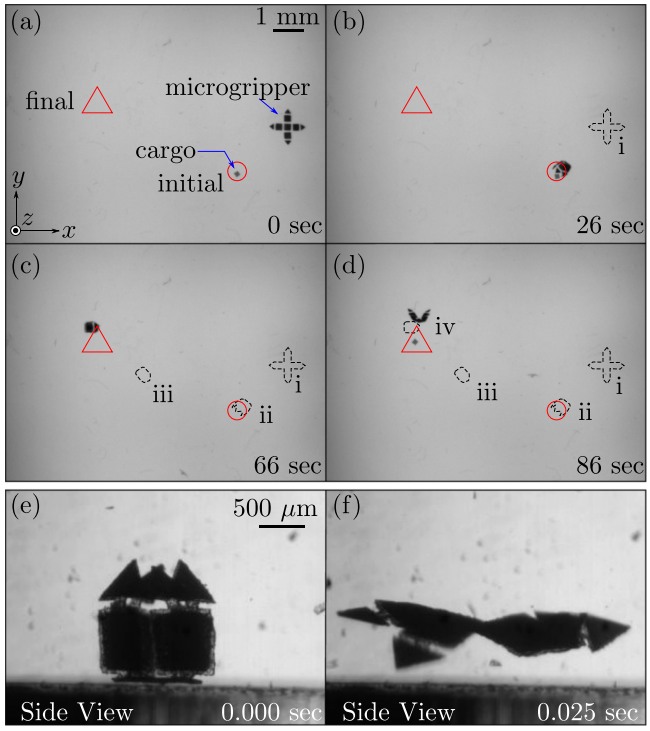

Figure 5. Experimental demonstrations of the microgripper. Four frames captured by a top-view camera during the pick-and-place experiment are shown chronologically in (a)–(d). The cargo's initial and final positions are marked out by a circle and a triangle, respectively. The path of the microgripper is illustrated by dashed contours in time instances of (i) 0 s, (ii) 26 s, (iii) 60 s, and (iv) 66 s. Two frames of the microgripper performing fast close-and-open motions at 20 Hz are shown in (e) and (f). Videos of the experiments are available in the supplementary material.

central workspace. The coils are powered by analog servo drives (30A8, Advanced Motion Controls), which receive inputs from a multifunction analog/digital I/O board (Model 826, Sensoray). Images of the workspace are captured by a 60 fps top-view camera (FO134TC, FOculus) and fed to a custom program, which interacts with the user through a graphical user interface and sends commands to the I/O board.

In the pick-and-place experiment shown in figures 5(a)–(d), the microgripper moves to the cargo, i.e., a 400 μm polymer cube, grasps it, transports it, releases it, and then moves away from it in the following procedures. (1) The microgripper is closed by the magnetic field applied along $+z$-axis. (2) The field changes its direction to the x–y plane with the microgripper always aligned with the field. Horizontal field gradient is applied to pull the microgripper until it has touched its cargo. Then the field gradient is removed and the microgripper stops. (3) The field strength is reduced to slightly open the microgripper, and the field direction changes to $-z$, rolling the microgripper to the top of its cargo. The magnetic field is then removed and re-applied to open

and close the microgripper, grasping the cargo to its hug. (4) Repeat step-2, but this time move the microgripper to the final position. (5) The magnetic field changes to $-z$ direction, then its strength is reduced to zero and the microgripper opens, releasing the cargo. (6) Lastly, the magnetic field is applied along $+z$ to bend the microgripper's limbs backwards. And the field direction gradually changes from $+z$ to $-z$, rolling the microgripper 180° and away from the cargo. In this experiment, the microgripper is pulled by magnetic field gradients that are smaller than 0.2 T m^{-1}. It has been stated previously that this microgripper can also roll on a substrate, because it is always aligned with the field direction by magnetic torques. Experiment is implemented to demonstrate this alternative locomotion method. Currents described by $i = \cos(2\pi ft)$ and $i = \sin(2\pi ft)$ are provided to x and z coils, respectively. The superposition of magnetic fields generated by x and z coils forms a uniform magnetic field in the x–z plane with a constant strength and a rotating direction at frequency f. This rotating field rolls the microgripper on the x–y plane and the video of this experiment is available in the supplementary material. Rolling is especially useful when the microgripper moves near a planar surface or get stuck by frictions.

Additionally, the microgripper is able to repeat fast close-and-open motions up to 20 Hz in water at room temperature, because no time-consuming responses are involved in its working principle. Frames of the microgrippers doing fast close-and-open motions are captured by a high-speed camera (IL3, Fastec Imaging) and shown in figures 5(e) and (f). The underlying principles of the microgripper are not reliant on the fluid properties of the operating media. Thus the microgripper still works in media with different viscosity and density. But different properties do have an effect on the microgripper's behavior. When the fluid density is different with the microgripper's density, which is estimated to be 1.6 g cc^{-1}, extra magnetic forces need to be applied to overcome the gravity or buoyancy, making 3D locomotion more difficult for the microgripper. The grasping speed of the microgripper is highly sensitive to the fluid drag, which is dependent on the viscosity. Higher viscosity value results in lower speed of the microgripper. A qualitative test is carried out in which the microgripper grasps in water and silicone oil with viscosity values of 20, 350, and 1000 cSt (25 °C). The microgripper still works, but its speed is inversely related to the fluid viscosity value. Results of this test is shown in the supplementary video, together with the two locomotion methods and the high-speed close-and-open motion of the microgripper.

5. Conclusion

In conclusion, we present the first 3D mobile microgripper that solely relies on magnetic forces and torques to work. With the magnetically-programmable material and a 3D symmetric four-limb structure, the microgripper has distinct characteristics. The orientation, shape, and position of the microgripper are directly controlled by the direction, strength, and spatial/temporal variance of the applied magnetic field, respectively. The microgripper has nonuniform stiffness and magnetization profiles along its body, with parts functioning as biological 'bones' and 'joints'. Experiments of the microgripper performing a pick-and-place task, two locomotion methods, and fast close-and-open motions are included to demonstrate the controllability of the microgripper. The microgripper is also tested in different fluids to show that it can work in environments with different properties. The working principles of the microgripper do not involve thermal responses, but it should be clarified that temperature does affect the microgripper's behavior by altering the properties of its operating media and the microgripper's materials. For example, changing temperature can increase or decrease the viscosity of the working fluid, which affects the microgripper's speed, as shown in the experiment section. If the temperature goes too high, it will degrade the microgripper's material and demagnetize the magnetic particles, disabling the microgripper's functionalities. In current research stage, the microgripper only operates in the range from room temperature (20 °C) to human body temperature (37 °C). We have not been able to observe any effect of temperature on the microgripper's behavior in this range. Considering that the microgripper works in aqueous mediae and does not rely on any thermal or chemical responses, the microgripper has the potential to be applied in biomedical tasks such as minimally invasive surgery, targeted drug delivery, and manipulation of individual cells or tissue structures. Moreover, the microgripper can also be used for the assembly of microstructures, whose gravitational forces are reduced by the environmental fluids. The manual operation involved in the fabrication of the microgripper limits the microgripper to be further downscaled. Thus, an integrated automatic fabrication process will be investigated in future research. Occasionally, the microgripper cannot open after closing, which is possibly a result of the local interactions between its fingers. Coatings will be applied to the fingers of the microgripper to prevent them from sticking to each other and make the grasping of the microgripper more robust. Governed by magnetic forces and torques, the microgripper is expected to exhibit similar behaviors at smaller scales, and will have potential applications in biomedical, microfluidic, and microrobotic tasks.

Acknowledgments

This work was supported by the Natural Sciences and Engineering Research Council of Canada (NSERC) through the Discovery Grant.

References

[1] Fusco S *et al* 2015 *ACS Appl. Mater. Interfaces* **7** 6803–11
[2] Kei Cheang U, Lee K, Julius A A and Kim M J 2014 *Appl. Phys. Lett.* **105** 083705
[3] Nelson B, Kaliakatsos I and Abbott J 2010 *Annu. Rev. Biomed. Eng.* **12** 55–85

[4] Chatzipirpiridis G, Ergeneman O, Pokki J, Ullrich F, Fusco S, Ortega J A, Sivaraman K M, Nelson B J and Pané S 2015 *Adv. Healthcare Mater.* **4** 209–14
[5] Martel S 2013 *Int. J. Adv. Robot. Syst.* **10** 30
[6] Diller E and Sitti M 2014 *Adv. Funct. Mater.* **24** 4397–404
[7] Chung S E, Dong X and Sitti M 2015 *Lab Chip* **15** 1667–76
[8] Walker R, Gralinski I, Keong Lay K, Alan T and Neild A 2012 *Appl. Phys. Lett.* **101** 163504
[9] Vasudev A and Zhe J 2008 *Appl. Phys. Lett.* **93** 103503
[10] Diller E D, Miyashita S and Sitti M 2012 *RSC Adv.* **2** 3850–6
[11] Diller E D, Giltinan J, Lum G Z, Ye Z and Sitti M 2015 *Int. J. Robot. Res.* **35** 114–28
[12] Zhang J, Jain P and Diller E 2016 Independent control of two millimeter-scale soft-bodied magnetic robotic swimmers *IEEE Int. Conf. on Robotics and Automation* pp 1933–8
[13] Mahoney A, Nelson N, Peyer K, Nelson B and Abbott J 2014 *Appl. Phys. Lett.* **104** 144101
[14] Diller E, Giltinan J, Jena P and Sitti M 2013 *Int. J. Robot. Res.* **32** 614–31
[15] Zhang J and Diller E 2015 Millimeter-scale magnetic swimmers using elastomeric undulations *IEEE/RSJ Int. Conf. on Intelligent Robots and Systems (Hamburg, Germany)* pp 1706–11
[16] Diller E, Zhuang J, Lum G, Edwards M and Sitti M 2014 *Appl. Phys. Lett.* **104** 174101
[17] Yamanishi Y, Sakuma S, Onda K and Arai F 2010 *Biomed. Microdevices* **12** 745–52
[18] Barbot A, Decanini D and Hwang G 2016 *Sci. Rep.* **6** 19041
[19] Tasoglu S, Diller E, Guven S, Sitti M and Demirci U 2014 *Nat. Commun.* **5** 3124
[20] Ye Z, Diller E and Sitti M 2012 *J. Appl. Phys.* **112** 064912
[21] Kuo J C, Tung S W and Yang Y J 2014 *Sensors Actuators* A **211** 121–30
[22] Breger J C, Yoon C, Xiao R, Kwag H R, Wang M O, Fisher J P, Nguyen T D and Gracias D H 2015 *ACS Appl. Mater. Interfaces* **7** 3398–405
[23] Randhawa J S, Leong T G, Bassik N, Benson B R, Jochmans M T and Gracias D H 2008 *J. Am. Chem. Soc.* **130** 17238–9